Journal of Organometallic Chemistry, 472 (1994) 337–345

Synthesis, structure and reactivity of binuclear rhodium dicationic carbonyl complexes *

Faisal Shafiq and Richard Eisenberg

Department of Chemistry, University of Rochester, Rochester, NY 14627 (USA)

(Received November 23, 1993; in revised form January 31, 1994)

Abstract

The reaction of $Rh_2(CO)_3(dppm)_2$ (**1**) with an excess of triflic acid, HSO_3CF_3, yields the dicationic tricarbonyl complex $Rh_2(CO)_3(dppm)_2^{+2}$ (**3**). Complex **3** is fluxional and undergoes terminal and bridging CO exchange as well as coordination and dissociation of $CF_3SO_3^-$ in solution. The crystal structure of the η^1-acetone complex $Rh_2(\eta^1\text{-}OC(CH_3)_2)(\mu\text{-}CO)(CO)(SO_3CF_3)(dppm)_2^+$ (**4**) has been determined. Complex **4** crystallizes in the triclinic space group $P\bar{1}$ as its triflate salt with a benzene of crystallization in a unit cell of dimensions $a = 12.087(4)$ Å, $b = 15.268(4)$ Å, $c = 20.602(4)$ Å, $\alpha = 87.06(2)$, $\beta = 73.61(2)$, $\gamma = 72.56(2)°$, $V = 3477.7$ Å^3 and $Z = 2$. Complex **4** possesses a binuclear structure in which the Rh centers are bridged by two dppm ligands and an asymmetrically bound CO ligand. The Rh–Rh bond distance is 2.778(2) Å while the Rh–O(acetone) distance is 2.09(1) Å. The Rh–O(triflate) distance is 2.37(1) indicating a weak interaction. Complex **3** reacts readily and reversibly under a CO atmosphere to form the tetracarbonyl complex $Rh_2(CO)_4(dppm)_2^{+2}$ (**5**). Upon heating under vacuum, complex **3** undergoes facile CO loss to form the dicarbonyl species $Rh_2(\mu\text{-}SO_3CF_3)(CO)_2(dppm)_2^+$ (**6**), *in situ*. Complex **6** is thought to possess an A-frame structure with triflate coordinated in the bridgehead position. Complex **3** promotes H/D exchange with acetone-d_6 and catalyzes the hydrogenation of acetone under 3 atm of H_2 at 70°C at the rate of 1 turnover per day. The reaction of **3** with H_2 leads to the generation of a moderately strong Bronsted acid whereas complex **5** reacts with H_2 to produce the known cationic species $Rh_2(\mu\text{-}H)(\mu\text{-}CO)(CO)_2(dppm)_2^+$ (**2**).

Key words: Rhodium; A-frame complexes; Protonation; Binuclear

1. Introduction

The chemistry of binuclear dppm (dppm = bis(diphenylphosphino)methane) bridged systems is well established [1–17]. Of particular interest to us and others is the reactivity of rhodium based systems with small molecules such as H_2, olefins and CO [13,15–23]. Recent activities have focused on the synthesis and reactivity of cationic binuclear complexes with the objective of promoting electrophilic activation of substrates by these systems in addition to their more usual oxidative addition chemistry. Studies describing the formation of cationic systems have been reported in the reactions of the tricarbonyl complex $Rh_2(CO)_3(dppm)_2$ (**1**) with HPF_6 and $CH_3SO_3CF_3$. The reaction with methyl triflate ($CH_3SO_3CF_3$) has been shown to produce the cationic A-frame complex $Rh_2(\mu\text{-}CH_3CO)(CO)_2(dppm)_2^+$ which undergoes facile and reversible CO deinsertion [22]. Complex **1** also reacts readily with one equivalent of HPF_6 to yield the binuclear cationic complex $RH_2(\mu\text{-}H)(\mu\text{-}CO)(CO)_2(dppm)_2^+$ (**2**) which was shown to be active in catalysis of both hydroformylation and the water-gas-shift reaction [20].

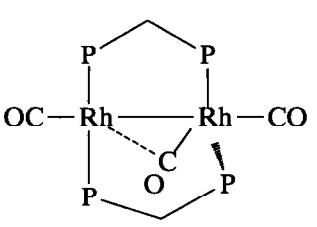

1

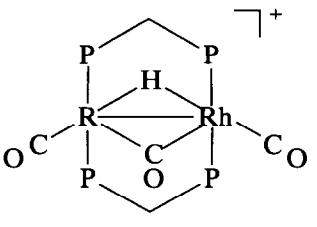

2

The present work details the synthesis and reaction chemistry of related dicationic species obtained by the

Correspondence to: Professor R. Eisenberg.

* Dedicated to Professor Helmut Werner on the occasion of his 60th birthday.

0022-328X/94/$7.00
SSDI 0022-328X(94)24577-6

reaction of dppm-bridged rhodium complexes with triflic acid. Specifically, we report that both complex **1** and **2** react independently with triflic acid to yield the dicationic tricarbonyl species $Rh_2(CO)_3(dppm)_2^{2+}$ (**3**) *via* protonation and subsequent H_2 elimination. The reactivity of complex **3** with acetone, CO, Et_2O, THF, H_2 and ethylene is also presented.

2. Experimental details

2.1. Materials, methods and preparations

Rhodium trichloride trihydrate (Johnson-Matthey) and the ligand bis(diphenylphosphino)methane (dppm) (Strem) were used as received without further purification. The starting complexes $Rh_2(CO)_3(dppm)_2$ [17], $Rh_2Cl_2(CO)_2(dppm)_2$ [24], $Rh_2(\mu\text{-}H)(\mu\text{-}CO)(CO)_2(dppm)_2^+$ [20] and $Rh_2(\mu\text{-}CH_3CO)(CO)_2(dppm)_2^+$ [22] were prepared according to published procedures. All syntheses were performed under N_2 using standard Schlenck and inert atmosphere techniques. All solvents used were of reagent grade and were dried and degassed before use. THF-d_8 was dried with Na-benzophenone ketyl and vacuum distilled. Acetone-d_6 and CD_2Cl_2 were dried with P_2O_5 and CaH_2, respectively, prior to vacuum distillation. Infrared spectra were obtained on a Mattson 6020 Galaxy series FTIR spectrometer. ^1H and $^{31}P\{^1H\}$ NMR spectra were recorded on a Bruker AMX-400 spectrometer at 400.13 and 161.92 MHz, respectively. ^{19}F NMR spectra were recorded on a Variant VXR-500 spectrometer at 470.38 MHz. Chemical shifts for ^1H NMR are reported in ppm downfield from tetramethylsilane, but were measured relative to residual ^1H resonances in the deuterated solvents ($CD_3C(O)CD_2H$, δ 2.04 ppm; $CHDCl_2$, δ 5.32 ppm; C_6D_5H, δ 7.15 ppm; THF-d_7, δ 3.65 ppm). $^{31}P\{^1H\}$ chemical shifts are reported in ppm downfield from phosphoric acid and were referenced relative to external 85% H_3PO_4. $^{19}F\{^1H\}$ chemical shifts are reported downfield from $CFCl_3$. Conductivity measurements were performed with a Yellow Springs Instruments (YSI) conductivity cell (no. 3401) and bridge model 31.

2.2. $[Rh_2(\mu\text{-}CO)(CO)_2(dppm)_2](CF_3SO_3)_2$ (3)

Method A. In a 50 ml round bottom flask, 0.200 g (184 μmol) of $Rh_2(CO)_3(dppm)_2$ (**1**) was dissolved in 10 ml of CH_2Cl_2 under an inert atmosphere. Neat HSO_3CF_3 (81 μl, 922 μmol) was injected into the solution which was stirred at room temperature for 30 min. The dark red solution of $Rh_2(CO)_3(dppm)_2$ (**1**) reacted with excess acid to produce a solution that changed from green to yellow and yielded a precipitate within 15 min. Any additional dissolved complex precipitated upon the addition of excess hexanes or Et_2O and can be filtered in air. Yield > 90%. Spectroscopic data: ^1H NMR (CD_2Cl_2): δ 4.23 (very broad; 4H; dppm $-CH_2-$), δ 7.32–7.49 ppm (40 H; dppm phenyl H). $^{31}P\{^1H\}$ NMR: δ 29.38 ppm (J(Rh–P) = 94.6 Hz). IR (KBr): ν(CO) = 2004 (terminal CO), 1969 (terminal CO), 1837 (semibridging CO) cm^{-1}. $^{13}C\{^1H\}$ NMR (233 K): δ 181.9 (terminal CO). Anal. Found: C, 48.39; H, 3.21. $Rh_2P_4C_{55}H_{44}O_9S_2F_6$ calcd.: C, 48.69; H, 3.27%. Conductivity: (Λ (10^{-4} M) = 197 Ω^{-1} cm^2 equiv^{-1}, acetone solution).

Method B. In a 50 ml round bottom flask, 0.100 g (89 μmol) of $Rh_2Cl_2(CO)_2(dppm)_2$ [24] was suspended in 10 ml of CH_2Cl_2 under a CO atm. $AgSO_3CF_3$ (0.228 g, 890 μmol) was added *via* a side arm adapter and stirred at room temperature for 30 min. A pale yellow solution formed as complex **1** reacted with the $AgSO_3CF_3$. The solution was filtered to remove AgCl and then evaporated until a yellow precipitate of **3** was deposited. The solid can be filtered in air and isolated in > 90% yield.

Method C. In an NMR tube, 0.010 g (8 μmol) of $Rh_2(\mu\text{-}CH_3CO)(CO)_2(dppm)_2$ [22] was dissolved in CD_2Cl_2 under 1 atm of CO. In the dry box, 3 μl of HBF_4 was added. An immediate color change from orange to yellow was observed. By ^1H NMR spectroscopy, the formation of acetaldehyde and complex **5** was observed. After the sample was evacuated, the ^1H NMR spectrum showed the formation of complex **3**.

Method D. In an NMR tube, 0.010 g (8 μmol) of $Rh_2(\mu\text{-}H)(\mu\text{-}CO)(CO)_2(dppm)_2^+$ [20] was dissolved in CD_2Cl_2 under 1 atm of CO. In the dry box, 3 μl of HBF_4 was added. An immediate color change from red to yellow was observed. After the sample was evacuated, the ^1H NMR spectrum shows the formation of complex **3**.

2.3. In situ generation of $[Rh_2(CO)_4(dppm)_2](CF_3SO_3)_2$ (5)

In an NMR tube, 0.010 g (8 μmol) of $Rh_2(CO)_3(dppm)_2^{2+}$ was dissolved in CD_2Cl_2 and placed under 1 atm of CO. The solution turned to pale yellow as the sample thawed prior to NMR analysis. ^1H NMR (acetone-d_6): δ 5.13 (singlet; 4 H; dppm $-CH_2-$), δ 7.40–7.77 ppm (40 H; dppm phenyl H). $^{31}P\{^1H\}$ NMR: δ 27.38 ppm. IR (CH_2Cl_2): ν(CO) = 1991 cm^{-1}. Conductivity: Λ (10^{-4} M) = 161 Ω^{-1} cm^2 equiv^{-1} (acetone solution).

2.4. Generation of $[Rh_2(\mu\text{-}SO_3CF_3)(CO)_2(dppm)_2](CF_3SO_3)$ (6)

In a 100 ml round bottom flask, 0.200 g (147 μmol) of $Rh_2(CO)_3(dppm)_2^{+2}$ (**3**) was dissolved in 20 ml of CH_2Cl_2 and stirred under an H_2 purge at room temperature until all of the solvent was evaporated. Com-

plex **6** was isolated as an impure solid in 70% yield. ^{1}H NMR (CD_2Cl_2): δ 4.21 (multiplet; 2 H; dppm $-CH_2-$); 3.50 ppm (multiplet; 2 H, dppm $-CH_2-$). $^{31}P\{^1H\}$ NMR: δ 19.79 ppm. IR (CH_2Cl_2): ν(CO) = 1965 cm^{-1}.

2.5. Reaction of 3 with $NaBH_4$ / CO

In a 50 ml round bottom flask, 0.200 g (147 μmol) of $Rh_2(CO)_3(dppm)_2^{+2}$ (**3**) was suspended in 10 ml of MeOH under a CO atmosphere. $NaBH_4$ (0.025 g, 925 μmol) was added *via* a side arm adapter to the complex. Complex **1** was deposited immediately as an orange/red solid. Spectroscopic data matched previously published results [17].

2.6. Reaction of 3 with CO / H_2 in acetone-d_6

In an NMR tube, complex **5** was generated by dissolving 0.010 g (8 μmol) of complex **3** in acetone-d_6 under 1200 Torr CO. Excess CO was removed by evacuation and the solution is placed under 1 atm of H_2. Within 20 min at room temperature, complete conversion to complex **2** was observed along with the liberation of a small amount of HD. Characteristic ^{1}H and $^{31}P\{^1H\}$ NMR resonances for complex **2** match those of an authentic sample [20].

2.7. Reaction of 3 with H_2 in acetone-d_6

In an NMR tube, 0.010 g (8 μmol) of complex **3** was dissolved in acetone-d_6. The sample was placed under 3 atm of H_2. By ^{1}H NMR spectroscopy an increase in the intensity of the acetone solvent peak was observed at the rate of about 3.5 turnover per day at room temperature. The increase in the intensity of the acetone peak was measured relative to that of cyclohexane which was added as an internal standard.

2.8. Reaction of 3 with H_2 / acetone in CD_2Cl_2

In an NMR tube, 0.010 g (8 μmol) of complex **3** was dissolved in CD_2Cl_2 to which 3 μl of acetone-H_6 was added. The sample was placed under 3 atm of H_2. By ^{1}H NMR spectroscopy, the formation of isopropanol was observed upon heating the sample at 70°C over a period of days at the rate of ~ 1 turnover per day. The production of isopropanol was established by ^{1}H NMR spectroscopy.

2.9. Reaction of 3 with D_2 / acetone

The same procedure as that used in the reaction of **3** with H_2 and acetone was followed. By ^{1}H NMR spectroscopy, the formation of isopropanol was observed upon heating the sample to 70°C over a period of days at the rate of ~ 1 turnover per day.

2.10. Reaction of 3 with H_2 / Et_2O in CD_2Cl_2

In an NMR tube, 0.010 g (8 μmol) of complex **3** was dissolved in CD_2Cl_2 to which was added 1 μl of diethyl ether. The ^{1}H NMR spectrum was recorded in which the ether resonances were observed at δ 3.434 and 1.15 ppm. The sample was then placed under 3 atm of H_2. The ^{1}H NMR spectrum exhibited ether resonances that were shifted significantly from where they were observed without H_2 (δ 3.50 and 1.18 ppm).

2.11. Reaction of 3 with H_2 / THF

In an NMR tube, 0.010 g (8 μmol) of complex **3** was dissolved in 0.5 ml of THF. The sample was then placed under 3 atm of H_2 whereupon all of the undissolved yellow starting material reacted to produce a dark red/brown solution. After 24 h at room temperature, a significant increase in solvent viscosity was noted and by 48 h the sample had formed a gel. The control sample (no added H_2) did not change over the same time period.

2.12. X-Ray structure determination of $[Rh_2(\eta^1\text{-}OC(CH_3)_2)(\mu\text{-}CO)(CO)(SO_3CF_3)(dppm)_2](CF_3SO_3) \cdot 1/2\ C_6H_6$ (4)

Orange crystals of complex **4** were grown from acetone/Et_2O solution. A crystal of complex **4** with dimensions (0.4 × 0.4 × 0.5 mm) was attached with epoxy to a glass fiber on a goniometer head. Crystal data and data collection parameters are summarized in Table 1. The initial cell determination was carried out using 25 centered reflections from different parts of reciprocal space with θ between 5 and 13°. The cell was determined using the Enraf-Nonius CAD4-SDP peak search, centering and indexing programs. The intensity data showed no evidence of decay during the course of data collection. Heavy atom methods were employed to locate the rhodium atoms and the DIRDIF program was used for structure expansion. Subsequent cycles of least squares refinements and difference Fourier maps located the remaining non-hydrogen atoms. After isotropic refinement, an empirical absorption correction (DIFABS) was applied [25]. In the final refinement of complex **4**, all of the non-hydrogen atoms except those of the triflate anion and the solvent of crystallization were defined by anisotropic thermal parameters. The supplementary material contains final positional and thermal parameters, calculated hydrogen positional parameters and complete tabulations of bond distances and angles (available from the authors).

3. Results and discussion

3.1. Reaction of $Rh_2(CO)_3(dppm)_2$ (1) with HSO_3CF_3

Reaction of a red solution of the tricarbonyl complex $Rh_2(CO)_3(dppm)_2$ (**1**) with an excess of triflic acid, HSO_3CF_3, in either CD_2Cl_2 or THF solution leads to an immediate color change to green and then to yel-

TABLE 1. Summary of crystallographic data for complex **4**

	4
Empirical formula	$C_{60}F_6H_{53}O_9P_4Rh_2S \cdot 1/2C_6H_6$
Crystal system	Triclinic
Space group	$P\bar{1}$
Z	2
a (Å)	12.087(4)
b (Å)	15.268(4)
c (Å)	20.602(4)
α (°)	87.05(2)
β (°)	73.61(2)
γ (°)	72.55(2)
V (Å^3)	3477.7
d_{calc} (g cm^{-3})	1.3615
T (°C)	−20.0
Diffractometer	Enraf-Nonius CAD4
$\lambda_{Mo\text{-}K\alpha}$ (graphite monochromated radiation)	0.71069
Scan type	$2\theta-\omega$
Scan rate (° min^{-1})	2–16.5
Total background time	Scan time/2
Take-off angle (°)	2.6
Scan range (°)	$0.7+0.35\tan\theta$
2θ range (°)	$4<2\theta<38$
Data collected	$+h, \pm k, \pm l$
No. of data collected	6878
No. of unique data $>3\sigma$	4822
No. of parameters varied	713
Absolute coefficient (cm^{-1})	6.768
Systematic absences	None
Range of transm factors	0.875–1.106
Equivalent data	$0kl, 0\bar{k}\bar{l}$
Agreement of equivalent data (F_o)	0.02
R_1	0.059
R_2	0.084
Goodness of fit	3.20
Largest peak in final E map	1.24

$R_1=\{\Sigma\|F_o|-|F_c\|\}/\{\Sigma|F_o|\}$; $R_2=[\Sigma w(|F_o|-|F_c|)^2]^{1/2}/\{\Sigma wF_o^2\}$, where $w=[\sigma^2(F_o)+(\rho F_o^2)^2]^{1/2}$ for the non-Poisson contribution weighting scheme. The quantity minimized was $\Sigma w(|F_o|-|F_c|)^2$. Source of scattering factors f_o, f', f'': D.T. Cromer and J.T. Waber, *International Tables for X-Ray Crystallography*, Kynoch Press, Birmingham, UK, 1974, Vol. IV, Tables 2.2B and 2.3.1.

low. Upon addition of hexanes or Et_2O saturated with CO, a yellow solid precipitates and is filtered in air. The green intermediate was not characterized. The yellow solid corresponding to **3** is very soluble in acetone and MeOH, slightly soluble in CD_2Cl_2 and THF, and insoluble in Et_2O, C_6H_6 and hexanes. Borohydride reduction of **3** in a MeOH solution while under CO regenerates the starting tricarbonyl complex **1**. The ^1H NMR (CD_2Cl_2) spectrum of **3** exhibits an unusually broad resonance at δ 4.23 ppm assigned to the dppm $-CH_2-$ protons. The aryl region exhibits a single set of aryl resonances for the dppm phenyl protons. The $^{31}P\{^1H\}$ NMR spectrum shows a single second order pattern at δ 29.38 ppm with a separation of 94.6 Hz between the principal lines of the second order pattern indicating the equivalence of all four phosphorus nuclei. This large separation in the AA'A''A'''XX' second order pattern is assigned to $(|{}^1J(Rh-P)+{}^xJ(Rh-P)|)$ [6,20,26–33]. The room temperature ^{19}F NMR spectrum shows a sharp singlet at δ 134.28 ppm for the $CF_3SO_3^-$ counterion. The room temperature $^{13}C\{^1H\}$ NMR spectrum exhibits only a single carbonyl environment with a resonance in the terminal carbonyl region at δ 181.9 ppm. In contrast with the NMR results, which indicate a highly symmetric structure, the solid state IR spectrum (KBr) of **3** reveals two terminal ν(CO) *at* 2004 and 1969 cm^{-1} and a semibridging CO stretch at 1837 cm^{-1}, while the solution IR spectrum exhibits terminal CO stretches at 2019, 1987 and 1969 cm^{-1}, and the semibridging CO stretch at 1841 cm^{-1}.

The ^{13}C and ^{31}P NMR data, when considered in light of the infrared results, indicate that the new species is fluxional in solution on the NMR timescale. This conclusion, together with the observed 1:2 electrolyte behavior (Λ (10^{-4} M) = 197 Ω^{-1} cm^2 equiv^{-1}, CH_2Cl_2 solution), suggests that **3** is the dicationic complex $Rh_2(dppm)_2(CO)_3^{+2}$ which is formed *via* chemical oxidation of $Rh_2(CO)_3(dppm)_2$ (**1**) through protonation and subsequent H_2 loss. Complex **3** can be generated *via* alternative routes. Reaction of the known cationic complexes $Rh_2(\mu\text{-}CO)(\mu\text{-}H)(CO)_2(dppm)_2^+$ [20], and $Rh_2(\mu\text{-}CH_3CO)(CO)_2(dppm)_2^+$ [22] with excess HBF_4 under CO yield a species identified below that under vacuum loses CO to generate complex **3**. Chloride abstraction from the face-to-face square planar dimer $Rh_2Cl_2(CO)_2(dppm)_2$ [24] with $AgSO_3CF_3$ under CO also produces this species that leads to complex **3**. Slow recrystallization of **3** yields orange crystals of a cationic acetone adduct **4** that was examined crystallographically.

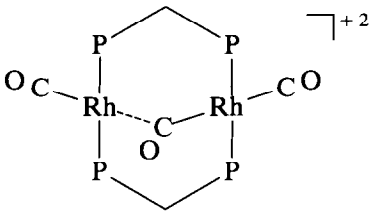

3

3.2. *Solid-state structure of* $Rh_2(SO_3CF_3)(\eta^1\text{-}OC(CH_3)_2)(\mu\text{-}CO)(CO)(dppm)_2^+$ (**4**)

Efforts to grow crystals of complex **3** produced orange crystals of a new species **4** not observed spectroscopically. An X-ray quality crystal was grown from an acetone/benzene solution and data were collected as

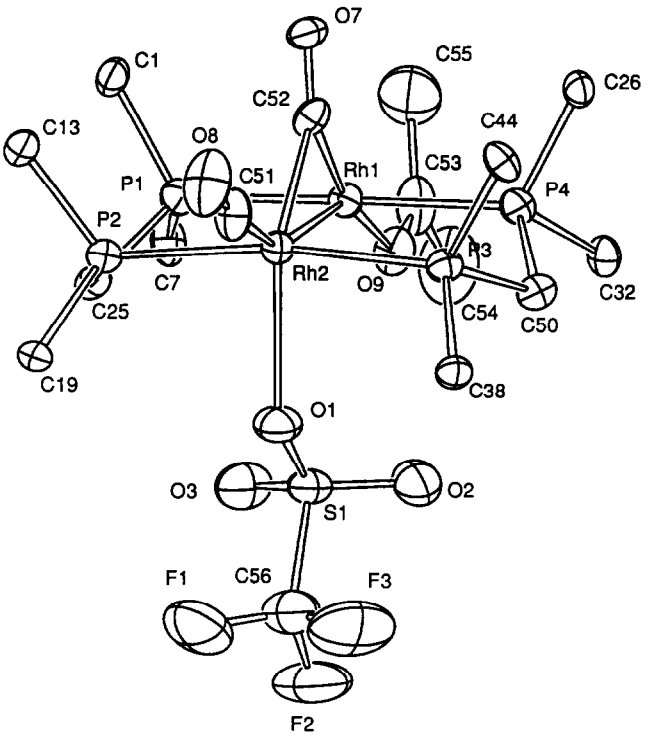

Fig. 1. A perspective view of $[Rh_2(\eta^1\text{-}OC(CH_3)_2(\mu\text{-}CO)(CO)(CF_3SO_3)(dppm)_2]^+$ (4) showing the oxygen bound acetone and the weakly coordinated $CF_3SO_3^-$. Only the *ipso* carbons of the dppm phenyl rings are shown. The uncoordinated $CF_3SO_3^-$ ion and the remaining phenyl carbons have been omitted for clarity. Thermal ellipsoids are set at 35% probability.

outlined in Table 1. The geometry of complex **4** is shown in the perspective drawing of Fig. 1, while selected intramolecular distances and angles are presented in Tables 2 and 3. The crystal structure consists of a well separated binuclear complex cation and its triflate anion. The molecular structure of **4** is that of a binuclear cationic complex with two dppm ligands and a single CO bridging the two Rh atoms. An oxygen bound acetone molecule is ligated to Rh_1 and a terminal CO is bound to Rh_2. The Rh_2–O_9 (acetone) distance is 2.09(1) Å. This distance is close in value to

TABLE 2. Intramolecular bond distances (Å) for $[Rh_2(\eta^1\text{-}OC(CH_3)_2(\mu\text{-}CO)(CO)(CF_3SO_3)(dppm)_2](CF_3SO_3)\cdot 1/2C_6H_6$ (4)

Rh1–Rh2	2.778(2)	Rh2–C52	2.06(2)
Rh1–P1	2.332(5)	S1–O1	1.44(1)
Rh1–P4	2.333(5)	S1–O2	1.42(1)
Rh1–O9	2.09(1)	S1–O3	1.42(1)
Rh1–C52	1.94(2)	O7–C52	1.15(2)
Rh2–P2	2.351(5)	O8–C51	1.13(2)
Rh2–P3	2.341(5)	O9–C53	1.22(2)
Rh2–O1	2.37(1)	C53–C54	1.53(3)
Rh2–C51	1.87(2)	C53–C55	1.47(3)

TABLE 3. Intramolecular bond angles (°) for $[Rh_2(\eta^1\text{-}OC(CH_3)_2(\mu\text{-}CO)(CO)(CF_3SO_3)(dppm)_2](CF_3SO_3)\cdot 1/2C_6H_6$ (4)

Rh2–Rh1–O9	148.3(3)	O1–S1–O3	115.1(8)
Rh2–Rh1–C52	47.8(5)	O1–S1–C56	101(1)
P1–Rh1–P4	176.2(2)	O2–S1–O3	116.5(9)
Rh1–Rh2–O1	94.8(3)	Rh2–O1–S1	133.9(7)
Rh1–Rh2–C51	153.6(6)	Rh1–O9–C53	131(1)
Rh1–Rh2–C52	44.3(5)	Rh2–C51–O8	172(2)
P2–Rh2–P3	170.0(2)	Rh1–C52–Rh2	87.9(8)
P3–Rh2–O1	87.4(3)	Rh1–C52–O7	139(1)
O1–Rh2–C51	111.6(7)	Rh2–C52–O7	133(1)
O1–Rh2–C52	139.1(6)	O9–C53–C54	119(2)
C51–Rh2–C52	109.3(8)	O9–C53–C55	122(2)
O1–S1–O2	113.8(8)		

other known Rh–O single bonds [22,34]. The phosphine donors at each Rh are mutually *trans* (P_1–Rh_1–P_4 = 176.2(2)°) and (P_2–Rh_2–P_3 = 170.0(2)°). The Rh–Rh separation of 2.778(2) Å is consistent with a Rh–Rh single bond and compares well with Rh–Rh single bond distances in $Rh_2(\mu\text{-}SiPhH)H_2(CO)_2(dppm)_2$ (2.813(1) Å), $Rh_2(\mu\text{-}CO)Br_2(dppm)_2$ (2.7566(8) Å), $Rh_2(\mu\text{-}CF_3C_2CF_3)Cl_2(dppm)_2$ (2.7447(9) Å), and $Rh_2(\mu\text{-}CO)(CO)_2(\mu\text{-}Cl)(dppm)_2^+$ (2.7838(8) Å) [30,35–37]. The bridging carbonyl is unsymmetrically positioned relative to the two Rh centers with a Rh_1–C_{52} distance of 1.94(2) Å and a Rh_2–C_{52} distance of 2.06(2) Å. The Rh_2–O_1 (triflate) bond distance of 2.37(1) Å is indicative of a very weak interaction between the triflate group and the metal center. Such a weak interaction suggests that rapid counterion coordination and dissociation are probable in solution. The low temperature behavior of complex **3** is discussed below in light of this X-ray data.

3.3. Fluxional behavior of 3

The fluxional behavior of **3** must account for the interconversion of terminal and semibridging CO ligands and lead to equivalence of the four dppm phosphines and the dppm $-CH_2-$ protons. The fluxionality of **3** was probed by low temperature NMR studies. At −45°C, the ^1H NMR spectrum of **3** exhibits two sets of inequivalent dppm $-CH_2-$ resonances while in the ^{31}P NMR spectrum two sets of resonances at δ 28.21 and δ 23.90 ppm and a single second order pattern at δ 28.52 ppm are observed. The ^{13}C NMR spectrum at −45°C exhibits resonances at δ 213.75, 190.60, 186.80, 184.15, 181.62 ppm. The most striking observation is the −45°C ^{19}F NMR spectrum in which two resonances at δ 134.64 (bound $CF_3SO_3^-$) and δ 133.43 ppm (free $CF_3SO_3^-$) are observed in a ratio of ~1:3, respectively. Upon warming the sample, resonances characteristic of **3** at room temperature are again observed. In light of the weakly bound triflate counterion seen in

the X-ray structure of complex **4**, we propose that the ^{19}F NMR spectrum of complex **3** indicates facile coordination/dissociation of the triflate counterion in solution and that this process can lead to equilibration of the carbonyl ligands and of the dppm phosphine donors. However, since the conductivity data for complex **3** in a CH_2Cl_2 solution is consistent with a 1:2 electrolyte formulation, the equilibrium shown below must lie to the left at room temperature.

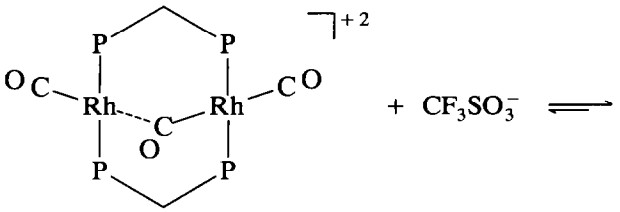

3

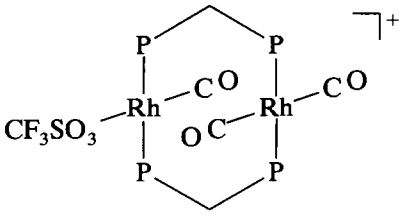

3a (1)

In repeated syntheses in acetone, **3** undergoes slow reaction with trace amounts of H_2O to form the known μ-OH A-frame species $Rh_2(\mu\text{-}OH)(dppm)_2$ first synthesized by Sharp *et al.* [34]. This decomposition is retarded in the presence of added ligands such as H_2, CO.

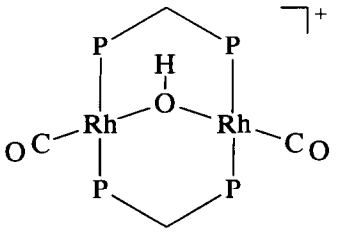

3.4. Reaction of 3 with H_2

Complex **3** reacts under 1–3 atm of H_2 in acetone-d_6 solution to generate *in situ* an unidentified dark red hydride species observed spectroscopically. The ^1H NMR spectrum exhibits a single set of resonances for the dppm aryl protons at δ 7.68, 7.44 and 7.37 ppm, a broad resonance at δ 4.28 ppm attributed to the dppm–CH_2– protons and a single broad hydride peak at δ −9.76 ppm. The hydride peak does not integrate well relative to the dppm methylene or aryl protons. The $^{31}P\{^1H\}$ NMR spectrum exhibits a single broad resonance at δ 28.36 ppm. This hydride species is stable at 70°C under H_2 for days without significant decomposition but it reverts cleanly and readily to complex **3** under vacuum. While the ^1H NMR spectrum of the hydride species remains unchanged for days, the residual acetone-d_5 solvent peak is observed to increase and broaden after 48 h at ambient temperature suggesting H/D exchange between acetone-d_6 and H_2. The rate of exchange is estimated at ~3.5 turnovers per day based on the intensity of the acetone-d_5 resonance relative to cyclohexane added as an internal standard.

In other solvents, similar reactivity with H_2 is observed. Although **3** is slightly soluble in CD_2Cl_2, it reacts completely with H_2 to produce a red/brown solution similar in appearance to that observed in acetone-d_6. By ^1H NMR spectroscopy, a broad resonance for the dppm –CH_2– protons at δ 3.66 ppm and a single set of aryl resonances for the dppm phenyl protons are observed. In addition, broad resonances centered at δ 4.58 ppm and 7.70 ppm are seen. By $^{31}P\{^1H\}$ NMR spectroscopy, a single unstructured resonance appears at δ 28.34 ppm. When **3** is placed under D_2 in the same solvent, the resonances at δ 4.58 and 7.70 ppm observed when **3** is placed under H_2 are not seen. We propose that the resonance at δ 4.58 ppm is due to free H_2 while the nature of the resonance at δ 7.70 ppm remains in question. When this species is placed under vacuum in either solvent, **3** is regenerated quantitatively. The sensitivity of this species to vacuum has precluded its isolation in pure form.

3.5. Reactivity of 3 under H_2

Upon heating a CD_2Cl_2 solution of **3** at 70°C under 3 atm of H_2 in the presence of ~20 equiv. of acetone, hydrogenation of acetone to isopropanol is observed at the rate of one turnover per day over a 3-day period. When the same reaction is carried out under 3 atm of D_2, a complicated resonance for the isopropanol methyl protons is observed indicative of deuterium incorporation into the methyl positions. In addition, when acetone-d_6 is added to a CD_2Cl_2 solution of complex **3** under 3 atm of H_2, the intensity of the free acetone peak increases. Complex **3** therefore catalyzes both acetone hydrogenation to isopropanol and H/D exchange of the methyl groups of free acetone. Bianchini has recently reported H/D exchange in acetone promoted by a molecular hydrogen complex of osmium [38]. We propose a similar scheme for our system as outlined in Scheme 1.

Due to the cationic nature of complex **3**, we propose that when it is placed under 3 atm of H_2, the hydride species formed *in situ* acts as a strong acid. In the case of acetone, the first step involves protonation of the ketone oxygen. For hydrogenation to isopropanol, a

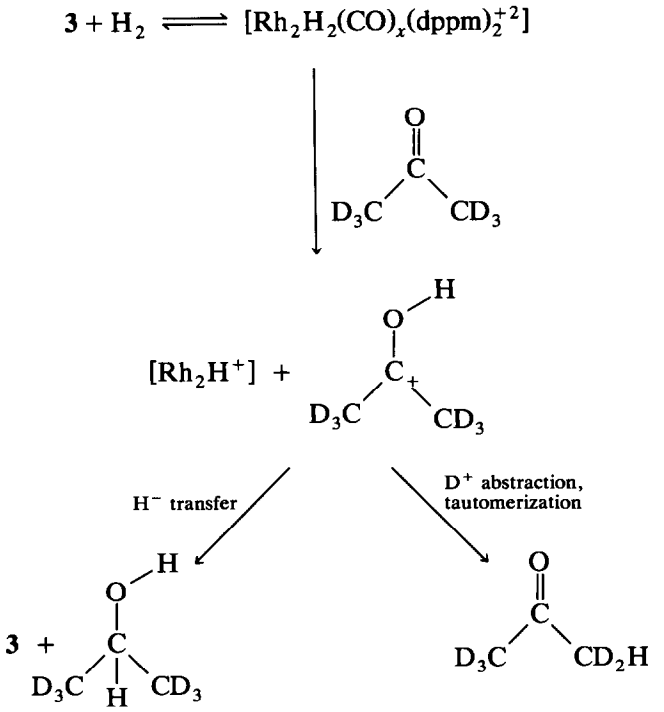

Scheme 1.

second hydrogen is then transferred as hydride to the carbenium ion, while for H/D exchange, proton loss and tautomerization follow the initial protonation. The ratio of products depends on the relative rates of the competing pathways. Observations suggest that the H/D exchange is faster than hydrogenation since the rate of H/D exchange with free acetone is ~4 turnovers per day compared with ~1 turnover per day for isopropanol formation. In either case, the reaction is relatively slow and may reflect the unfavorable nature of the second step in the transformations.

The reaction of complex **3** with H_2 in THF solvent provides an indication of the acidity of the unidentified hydride species. When a sample of complex **3** is dissolved in THF and placed under 3 atm of H_2, complete dissolution of undissolved material is observed. After 24 h at room temperature, a significant increase in the viscosity of the solution is observed, while after 48 h, the solvent has solidified. If an identical sample is prepared but is not placed under H_2, no change in solvent viscosity is observed. These observations suggest that the hydride species formed *in situ* is sufficiently acidic to protonate THF and catalyze ring opening polymerization. Similarly, we also find that when ~0.5 equiv. of Et_2O is added to a CD_2Cl_2 solution of **3** under 3 atm of H_2, the resonances due to the ether ethyl groups shift significantly from δ 3.43 and 1.15 ppm in the absence of H_2, to δ 3.50 and 1.18 ppm under H_2 consistent with protonation at oxygen.

3.6. Reaction of 3 with CO

The tricarbonyl complex $Rh_2(dppm)_2(CO)_3^{+2}$ (**3**) reacts immediately under 1 atm of CO to generate a new pale yellow species that is only observed *in situ*. Facile loss of CO under vacuum regenerates the tricarbonyl starting material **3**. By ^1H NMR spectroscopy in acetone-d_6, the pale yellow complex exhibits a single sharp dppm $-CH_2-$ resonance at δ 5.13 ppm while in the $^{31}P\{^1H\}$ NMR spectrum, a second order pattern is observed at δ 27.38 ppm, indicating equivalence of all four phosphorus nuclei. By IR spectroscopy, a single broad stretch is observed at 1991 cm^{-1} ($W_{1/2} = 60$ cm^{-1}), consistent with the presence of terminal CO ligands only; no stretches are seen in the bridging or semibridging CO region. Although two bands are expected, the broad nature of the CO stretch suggests that they overlap. In contrast to the ^{19}F NMR spectrum of complex **3**, the ^{19}F NMR spectrum of complex **5** shows a singlet at δ 136.00 ppm, which does not change significantly upon cooling. These results, together with the observed 1:2 electrolyte behavior (Λ (10^{-4} M) = 161 Ω^{-1} cm^2 $equiv^{-1}$, acetone solution), suggest the formation of the dicationic complex $Rh_2(dppm)_2(CO)_4^{+2}$ (**5**) in which both rhodium centers are square planar d^8 cations ligated by two mutually *trans* carbonyl ligands and two phosphine donors.

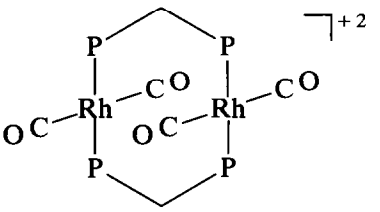

5

Complex **5** reacts within 10 min at room temperature under 1 atm of H_2 in acetone-d_6 or CD_2Cl_2 solvent to yield $Rh_2(\mu\text{-}H)(\mu\text{-}CO)(CO)_2(dppm)_2^+$ (**2**) [20] and a small amount of HD. It is worth noting that HD exchange between H_2 and acetone-d_6 is not catalytic; the intensity of the free HD resonance does not grow with time. CO thus appears to saturate the catalyst to preclude further reaction.

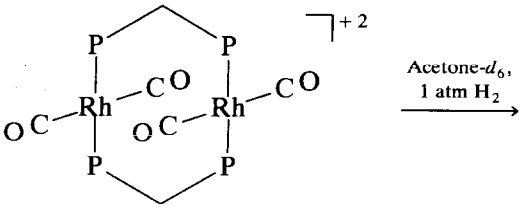

5

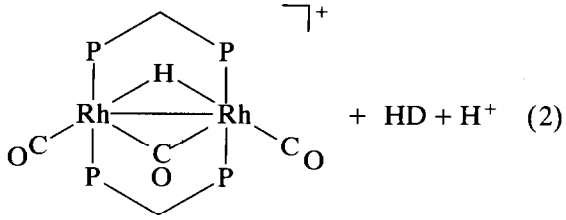

+ HD + H^+ (2)

2

3.7. Observation of $Rh_2(\mu\text{-}O_3SCF_3)(CO)_2(dppm)_2^+$ (6)

A CH_2Cl_2 solution of $Rh_2(dppm)_2(CO)_3^{2+}$ (**3**) reacts with H_2 to produce a dark red/brown solution (*vide supra*). However, when a CH_2Cl_2 solution of **3** is placed under a dynamic H_2 purge, the initial dark red solution slowly turns orange as CO is lost and removed from the system. As the remaining solvent is evaporated, an orange solid is isolated which contains a mixture of **3** and a new species. A CD_2Cl_2 solution of this orange solid exhibits ^1H NMR spectrum resonances at δ 4.21 and 3.50 ppm assigned to a set of inequivalent dppm $-CH_2-$ protons in addition to those assigned to complex **3**; no resonances in the hydride region are seen. The $^{31}P\{^1H\}$ NMR spectrum shows two second order patterns, one for **3** and one at δ 19.79 ppm indicating the equivalence of all four phosphorus nuclei. The solid state IR spectrum (KBr) exhibits a broad stretch at 1965 cm^{-1} in addition to those assigned to **3** while no new stretches are seen in the bridging or semibridging region. When this orange solid is dissolved in CD_2Cl_2 and placed under 1 atm of CO, **5** is generated quantitatively as evidenced by ^1H NMR spectroscopy. These spectroscopic features and reactivity with CO suggest the A-frame complex $Rh_2(\mu\text{-}O_3SCF_3)(CO)_2(dppm)_2^+$ (**6**) is formed *via* CO loss from **3**.

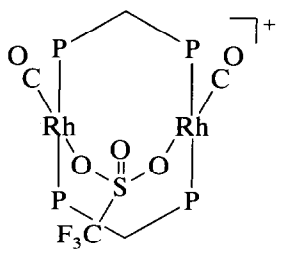

6

4. Conclusions

Reaction of $Rh_2(CO)_3(dppm)_2$ (**1**) with HSO_3CF_3 forms the dicationic tricarbonyl complex $Rh_2(CO)_3(dppm)_2^{+2}$ (**3**). $Rh_2(CO)_3(dppm)_2^{+2}$ (**3**) is in equilibrium with the triflate coordinated cation $Rh_2(CF_3SO_3)(CO)_3(dppm)_2^{+2}$ (**3a**). In acetone solvent, **3** undergoes CO substitution by the solvent to produce an oxygen bound acetone species **4**. The structure of the η^1-acetone adduct **4** confirms the ionic formulation of these complexes and supports facile triflate coordination and dissociation in solution based on the weak $Rh-O_1$ (triflate) bond observed structurally. Complex **3** reacts *in situ* with excess CO to produce the face to face square planar dimer $Rh_2(CO)_4(dppm)_2^{+2}$ (**5**). In CH_2Cl_2, **3** under H_2 reacts with added acetone to catalyze H/D exchange and hydrogenation to isopropanol. Complex **3** under H_2 also promotes ring opening polymerization of THF when it is used as a solvent. The reactivity of complex **3** under H_2 suggests that the ionic hydride species formed *in situ* is a strong Bronsted acid. Finally, complex **3** is observed to lose CO to form the triflate bridged species $Rh_2(\mu\text{-}CF_3SO_3)(CO)_2(dppm)_2^+$ (**6**).

Acknowledgements

We wish to thank NSF (CHE 89-09060) for financial support of this work and the Johnson Matthey Co. for a generous loan of rhodium trichloride. We also wish to thank Professor W.D. Jones for helpful discussions.

References

1 F. Antwi-Nsiah and M. Cowie, *Organometallics, 11* (1992) 3157.
2 A.L. Balch, C.-L. Lee, C.H. Lindsay and M.M. Olmstead, *J. Organomet. Chem., 177* (1979) C22.
3 A.L. Balch, L.S. Benner and M.M. Olmstead, *Inorg. Chem., 18* (1979) 2996.
4 D.H. Berry and R. Eisenberg, *Organometallics, 6* (1987) 1796.
5 M. Cowie and T.G. Southern, *Inorg. Chem., 21* (1982) 246.
6 M. Cowie, J.T. Mague and A.R. Sanger, *J. Am. Chem. Soc., 100* (1978) 3628.
7 B. Delavaux, B. Chaudret, N.J. Taylor, S. Arabi and R. Poilblanc, *J. Chem. Soc., Chem. Commun.*, (1985) 805.
8 Y.-W. Ge, F. Peng and P.R. Sharp, *J. Am. Chem. Soc., 112* (1990) 2632.
9 Y.-W. Ge and P.R. Sharp, *Inorg. Chem., 31* (1992) 379.
10 K.W. Kramarz and R. Eisenberg, *Organometallics, 11* (1992) 1997.
11 J.T. Mague and A.R. Sanger, *Inorg. Chem., 18* (1979) 2060.
12 L. Manojlovic-Muir, K.W. Muir, A.A. Frew, S.S.M. Ling, M.A. Thomson and R.J. Puddephatt, *Organometallics, 3* (1984) 1637.
13 R. McDonald, B.R. Sutherland and M. Cowie, *Inorg. Chem., 26* (1987) 3333.
14 P.R. Sharp and Y.-W. Ge, *J. Am. Chem. Soc., 109* (1987) 3796.
15 B.A. Vaartstra and M. Cowie, *Inorg. Chem., 28* (1989) 3138.
16 C. Woodcock and R. Eisenberg, *Inorg. Chem., 23* (1984) 4207.

17 C. Woodcock and R. Eisenberg, *Inorg. Chem., 24* (1985) 1285.
18 T.C. Eisenschmid, R.U. Kirss, P.P. Peutsch, S.I. Hommelthoft, R. Eisenberg, J. Bargon, R.G. Lawler and A.L. Balch, *J. Am. Chem. Soc., 109* (1987) 8089.
19 R.U. Kirss and R. Eisenberg, *Inorg. Chem., 28* (1989) 3372.
20 C.P. Kubiak, C. Woodcock and R. Eisenberg, *Inorg. Chem., 21* (1982) 2119.
21 B.A. Vaartstra, K.N. O'Brien, R. Eisenberg and M. Cowie, *Inorg. Chem., 27* (1988) 3668.
22 F. Shafiq, K. Kramarz and R. Eisenberg, *Inorg. Chim. Acta, 213* (1993) 111.
23 F. Shafiq and R. Eisenberg, *Inorg. Chem., 32* (1993) 3287.
24 J.T. Mague and J.P. Mitchener, *Inorg. Chem., 8* (1969) 119.
25 N. Walker and D. Stuart, *Acta Crystallogr., Sect. A 39* (1983) 158.
26 A.L. Balch, *J. Am. Chem. Soc., 98* (1976) 8049.
27 M. Cowie, J.T. Mague and A.R. Sanger, *J. Am. Chem. Soc., 100* (1978) 3628.
28 M. Cowie, S.K. Dwight and A.R. Sanger, *Inorg. Chim. Acta, 31* (1978) L407.
29 M. Cowie and S.K. Dwight, *Inorg. Chem., 19* (1980) 2500.
30 M. Cowie and R.S. Dickson, *Inorg. Chem., 20* (1981) 2682.
31 S.P. Deraniyagala and K.R. Grundy, *Inorg. Chim. Acta, 84* (1984) 205.
32 K.W. Kramarz, T.C. Eisenschmid, D.A. Deutsch and R. Eisenberg, *J. Am. Chem. Soc., 113* (1991) 5090.
33 C.P. Kubiak and R. Eisenberg, *J. Am. Chem. Soc., 102* (1980) 3637.
34 P.R. Sharp and J.R. Flynn, *Inorg. Chem., 26* (1987) 3231.
35 W.-D. Wang, S.I. Hommeltoft and R. Eisenberg, *Organometallics, 7* (1988) 2417.
36 M. Cowie and S.K. Dwight, *Inorg. Chem., 19* (1980) 2508.
37 M. Cowie, *Inorg. Chem., 18* (1979) 286.
38 C. Bianchini, K. Linn, D. Masi, M. Meruzzini, A. Polo, A. Vacca and F. Zanobini, *Inorg. Chem., 32* (1993) 2366.